ELSEVIER

International Journal of Adhesion & Adhesives 23 (2003) 383–392

International Journal of Adhesion & Adhesives

www.elsevier.com/locate/ijadhadh

Hot-melt adhesive properties of EVA/aromatic hydrocarbon resin blend

Young-Jun Park, Hyun-Joong Kim*

Laboratory of Adhesion and Bio-Composites, Department of Forest Products, Seoul National University, Suwon 441-744, South Korea

Accepted 13 May 2003

Abstract

A series of ethylene vinyl acetate copolymers (EVAs) were blended with aromatic hydrocarbon resins for use as hot-melt adhesives. The glass transition temperature, viscoelastic properties, melt viscosity, crystallinity and adhesion properties of the EVA/aromatic hydrocarbon resin system were determined as a function of the softening point of the aromatic hydrocarbon resin, the blend ratio of the two components and the vinyl acetate content of EVAs. Most blends showed a glass transition temperature at about −25°C and a melting peak between 30°C and 100°C. The peaks of loss modulus increased with increasing softening point of the aromatic hydrocarbon resin. The melt viscosity of the blends decreased with increasing temperature. Also, the melt viscosity increased with increasing softening point, but decreased with increasing aromatic hydrocarbon resin and vinyl acetate content. Increasing the softening point of the aromatic hydrocarbon resins, in cases of the same blend ratio, increased the crystallinity, while the addition of aromatic hydrocarbon resin decreased the crystallinity. Also, increasing the vinyl acetate content decreased the crystallinity of the blend, due to a decrease in the crystalline region of ethylene. The lap-shear strength increased with increasing softening point of the aromatic hydrocarbon resin. The lap-shear strength also increased with increasing concentration of aromatic hydrocarbon resin, until it reaches a maximum value.

Keywords: A. Adhesive for wood; A. Hot-melt; C. Dynamic mechanical analysis; C. Lap-shear

1. Introduction

Hot-melt adhesives have become very popular in the last decade because they are convenient and satisfy environmental requirements [1]. Hot-melt adhesives are 100% solid thermoplastic compounds that contain neither solvent nor an aqueous carrier for the active adhesive components [2]. These adhesives are solids at room temperature, but they liquidfied when heated to the temperature at which they are applied. When applied, hot-melts bond and cool rapidly. With the development of the petrochemical industry, various polymer materials and thermoplastics, such as ethylene vinyl acetate copolymers (EVAs), polyolefins, polyamides, polyurethane and polyesters, have formed the basis of hot-melt adhesives [5]. EVA has a wide range of melt index values and good adhesion to a variety of materials, and its price is low. Therefore, EVA is the most popular polymer used in hot-melt adhesives [6]. Generally, EVA for hot-melt adhesive has 18–40 wt% of vinyl acetate (VAc) content and its melt indices are 2–200 g/10 min [7]. Chemically, hydrocarbon resin streams may be classified as containing primarily aromatic, aliphatic and diene (cyclic olefin) monomers. Aromatic resins can be obtained with various softening points, from about 10°C to over 150°C, and excellent compatibility with SBR and EVA elastomers, and some of them are compatible with acrylate copolymers [8,9].

Dynamic mechanical analysis (DMA) has been widely used for investigating the structure and viscoelastic behavior of polymeric materials and for determining their relevant stiffness and damping characteristics for various applications. Several research groups have investigated the viscoelastic properties of EVA-based hot-melt adhesives [3–5]. Also, the rheological properties of hot-melt adhesives are an important consideration because they determine the processing conditions.

*Corresponding author. Tel.: +82-31-290-2601; fax: +82-31-293-9376.

E-mail address: hjokim@snu.ac.kr (H.-J. Kim).

0143-7496/03/$ - see front matter
doi:10.1016/S0143-7496(03)00069-1

In this paper, the miscibility and viscoelastic properties were measured and analyzed using DMA and differential scanning calorimetric (DSC) analyses of various blends of EVA/aromatic hydrocarbon resin system. The rheological properties of the system were investigated based on the variation of melt viscosity. Also, the crystallinity of the EVA/aromatic hydrocarbon resin system was determined by means of a wide-angle X-ray scattering study. Finally, the lap-shear strengths of the EVA-based hot-melt adhesives were examined using white birch as the adherend. The failure modes were classified as interfacial, interfacial-cohesive or cohesive failure.

2. Experimental

2.1. Materials

2.1.1. Polymers

EVAs were supplied by the Hanwha Chemical Corp., in Korea. Table 1 shows the VAc contents, melt indices and molecular weights of the EVAs.

2.1.2. Tackifiers

Aromatic hydrocarbon resins with different softening points were supplied by the Kolon Chemical Co., Ltd., in Korea. Table 2 indicates the softening points and molecular weights of the aromatic hydrocarbon resins.

2.1.3. Antioxidant

To reduce thermal degradation of the hot melt adhesives, 0.25 parts by weight of a phenolic antioxidant, Irganox 1010 (Ciba Geigy), was used as a thermal stabilizer.

2.1.4. Adherends used for measuring single lap-shear strength

White birch (moisture content: 8.67%) with dimensions of $101.6 \times 25.4\,mm^2$ was used to perform the single lap-shear test for the EVA-based hot-melt adhesives and its surface was sanded. The thickness of white birch adherend was 5 mm.

2.2. Experimental

2.2.1. Gel permission chromatography

2.2.1.1. Polymers. The molecular weights and molecular weight distributions (M_w/M_n) of the EVAs were measured using a Waters 150-CV (Shodex linear column, GPC HT-806 M). EVAs were maintained in an oven at 165°C for 1 h and then filtered. The solvent used was 1,2,4-trichlorobenzene. A refractive index detector was used.

2.2.1.2. Tackifiers. The molecular weights and molecular weight distributions (M_w/M_n) of the aromatic hydrocarbon tackifiers were measured using a Waters GPC (Column: HR-1, HR-2, HR-3, HR-4). The solvent used was tetrahydrofuran (THF). A refractive index detector was used. Polystyrenes with different molecular weight values were used as the calibration material.

2.2.2. Blend of polymer and tackifier

EVA-15, EVA-20 and EVA-28 were mixed with tackifier P-90, P-120 and P-140 in a 300 g internal mixer at 30 rpm with a machine temperature of 180°C. First, the tackifier and antioxidant were mixed. The quantity of antioxidant, Irganox 1010, was 0.25 parts. When the tackifier became masticated and formed a homogeneous melt, the EVA was slowly added until completion. The mixing time was about 20 min. EVA and tackifier were blended with various ratios of 7:3, 6:4, 5:5, 4:6 and 3:7. EVA-based hot-melt adhesive films were obtained by compression molding.

Table 2
Softening point and molecular weight of tackifier resins

Code	Softening Point	T_g(°C)[a]	M_n[b]	M_w[b]	MWD[b]	Commercial name
P-90	95±5.0	46	450	760	1.7	P-90
P-120	120±5.0	74	700	1400	2.1	P-120
P-140	145±5.0	106	1000	2300	2.3	P-140

[a] Measured by DSC.
[b] Measured by GPC.

Table 1
VAc content and melt index of EVA copolymer resins

Code	VAc. content (wt %)[a]	Melt index (dg/min)[b]	T_g(°C)[c]	M_n[d]	M_w[d]	MWD[d]	Commercial name
EVA-15	15.0	10.0	−29	19,000	161,000	8.4	EVA1152
EVA-20	20.0	20.0	−28	18,000	95,000	5.3	EVA1156
EVA-28	28.0	18.0	−27	19,000	85,000	4.5	EVA1159

[a] VAc, measured by elemental analyzer and FT-IR.
[b] ASTM D1238.
[c] Measured by DSC.
[d] Measured by GPC.

2.2.3. Differential scanning calorimetry

The glass transition temperature (T_g) was measured using a TA Instruments Q-100 differential scanning calorimeter (TA Instruments) at a heating rate of 10°C/min. The scanning cycles consisted of heating from room temperature to 200°C at 10°C/min, cooling from 200°C to −70°C by ice quenching, and then heating to 200°C again at a rate of 10°C/min. The results of the second run were used for this study.

2.2.4. Dynamic mechanical analysis

The viscoelastic properties of the hot-melt adhesives were measured using a TA Instruments DMA 2980 (TA Instruments) at a frequency of 10 Hz. The test temperatures were in the range of −100°C to 75°C with a heating rate of 5°C/min under liquid nitrogen.

2.2.5. Melt viscosity

Melt viscosity was measured using a Brookfield Viscometer Model DV-II+ with a Brookfield Thermosel System to accurately measure the melt viscosity at elevated temperatures of 160°C, 180°C and 200°C. A SC4-28 spindle was used to measure a viscosity range of 250–5,000,000 cP.

2.2.6. Wide angle X-ray scattering

WAXS measurements were carried out using a small-angle X-ray scattering (SAXS, NICEM at Seoul National University) with general area detector diffraction (GADDS) working at 40 kV and 45 mA with Ni-filtered CuKα radiation ($\lambda = 0.15405$ nm). Scans were made between Bragg angles of 0–38° with an exposure time of 180.01 s and the diffractive intensity was recorded every 0.01°.

2.2.7. Single lap-shear test

The adhesive joint was then obtained by pressing the film between two white birch adherend at a temperature of 180°C for 5 min at 27.8 psi of pressing. The bondline thickness was maintained at 0.1 mm. After the lap joints assembly, all of the substrates were conditioned for 24 h in a temperature and humidity chamber, in which a relative humidity of 50% at 30°C was maintained. Single lap-shear strength was measured using a Zwick Universal Testing Machine Z101 (NICEM at Seoul National University) at a crosshead speeds (CHS) of 300 mm/min and a temperatures of 25°C. Failure modes were noted as being interfacial, interfacial-cohesive and cohesive failures.

3. Results and discussion

3.1. Differential scanning calorimetry

The glass transition temperature measured by DSC is most widely used for determining the compatibility of polymer blends. It has usually been associated with the onset of segmental mobility in the amorphous phase of an amorphous or semicrystalline polymer. Figs. 1 and 2 show DSC thermograms of EVAs and aromatic hydrocarbon resins, respectively. All EVAs have glass transition temperatures between −25°C and −30°C. Fig. 1 shows that all EVAs exhibit marked heat absorption at 30–100°C. Chen et al. [10] have reported similar

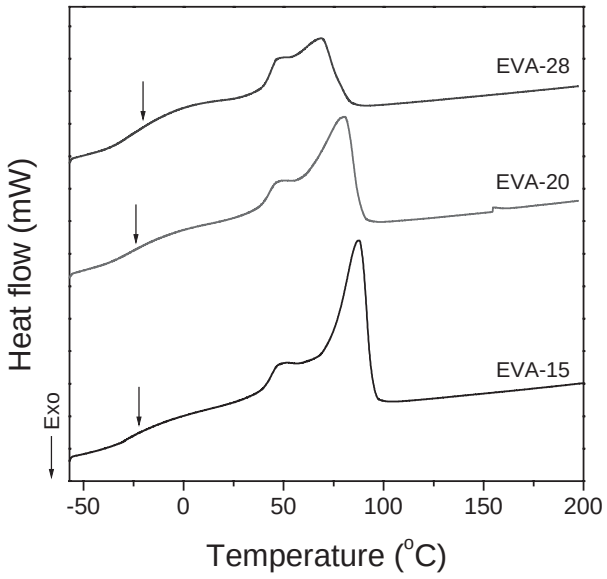

Fig. 1. DSC thermograms of EVA copolymers.

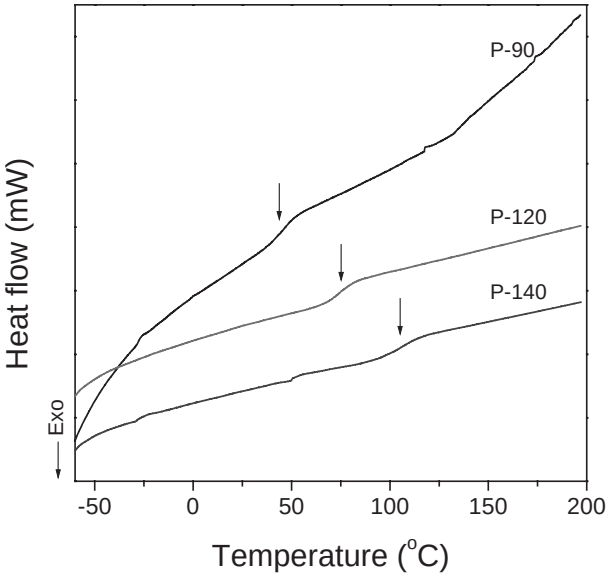

Fig. 2. DSC thermograms of aromatic hydrocarbon resins.

behavior in the case of polyesteramide. This behavior might be due to the hydrocarbon ring of the aromatic hydrocarbon resin and to the long hydrocarbon chain of the ethylene vinyl acetate group. Fig. 2 shows that the aromatic hydrocarbon resins, P-90, P-120 and P-140 have glass transition temperatures of about 46°C, 74°C and 106°C, respectively. The glass transition temperature of aromatic hydrocarbon resin increased with increasing softening point of that. Fig. 3 consists of DSC thermograms of each blend showing their different softening points. The glass transition temperature of the blend of EVA-20 with P-120 is observed at −25°C to −30°C, but it is difficult to identify the glass transition temperature for the other blends. Also, the heat of fusion of blends did not change as softening point of aromatic hydrocarbon resin increased. Fig. 4 shows the glass transition and the heat of fusion of EVAs, containing 50 wt% of P-120, as a function of the vinyl acetate content. The glass transition temperature changed slightly and heat of fusion decreased slightly with increasing vinyl acetate content, as shown in Fig. 4, because of decreasing crystallinity of EVAs. It is difficult to distinguish the miscible from the immiscible blends using the differential scanning calorimeter results shown in Figs. 3 and 4.

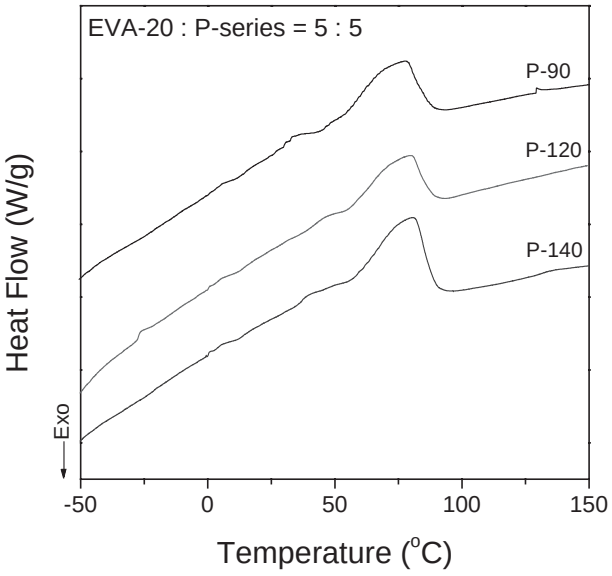

Fig. 3. DSC thermograms of the blend with different softening points.

3.2. Dynamic mechanical analysis

The mechanical properties of the polymers are highly dependent on temperature and on the time-scale of any deformation; these polymers are viscoelastic and exhibit some of the properties of both viscous liquids and elastic solids [11]. In dynamic mechanical analysis, the sample is deformed cyclically, usually under forced vibration conditions. By monitoring the stress–strain relationship while varying the temperature, information can be obtained about the relaxation behavior of the material being tested. DMA measurements were conducted in the temperature range from −100°C to 75°C, since higher temperatures caused the polymers to melt. As shown in Fig. 5, the storage modulus (E') of the blends varied drastically between 0°C and 25°C, and the loss modulus (E'') of the blends has peaks at 30°C, 27°C and 17°C for P-90, P-120 and P-140, respectively. In Fig. 6, the storage modulus of the blends varied drastically between 0°C and 25°C, and the loss modulus of the blends shows peaks at 17°C, 20°C, 27°C, 26°C and 27°C for the blend ratios of 7:3, 6:4, 5:5, 4:6 and 3:7, respectively.

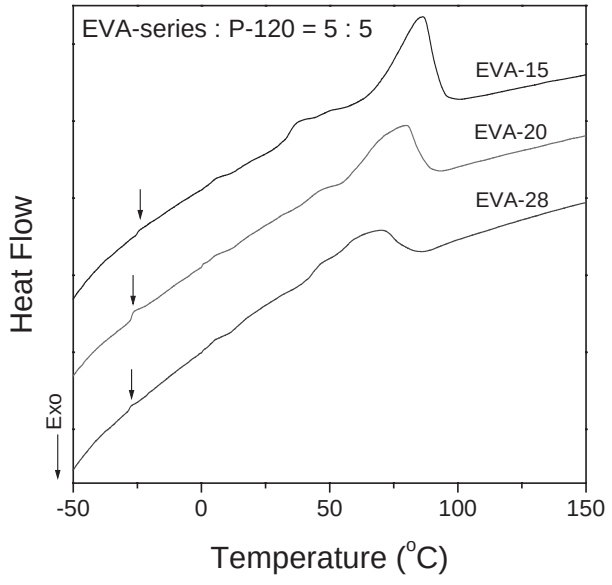

Fig. 4. DSC thermograms of the blend with different VAc contents.

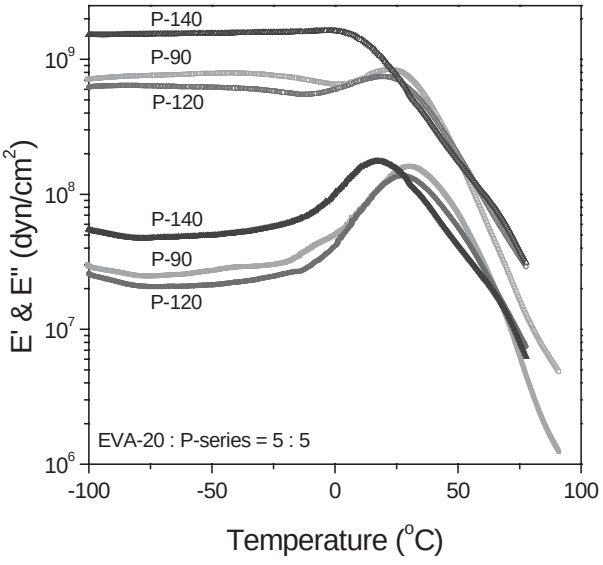

Fig. 5. Storage modulus (E') and loss modulus (E'') vs. temperature for blends of EVA-20 with 50 wt% of P-90, P-120 and P-140.

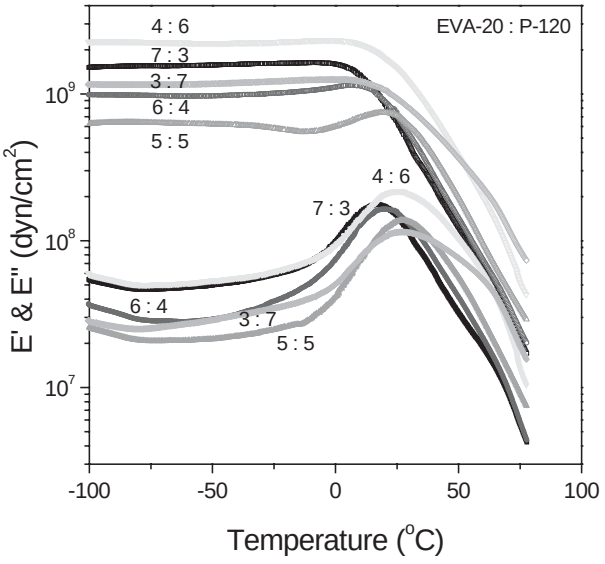

Fig. 6. Storage modulus (E') and loss modulus (E'') vs. temperature of blends of EVA-20 with P-120 as a function of the blend ratio.

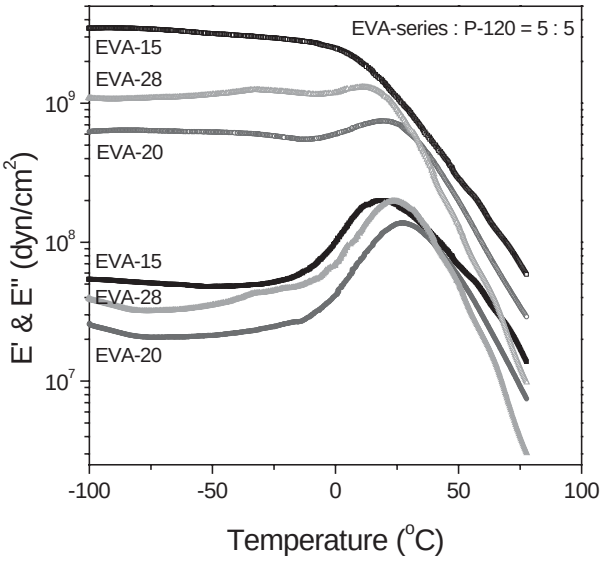

Fig. 7. Storage modulus (E') and loss modulus (E'') vs. temperature of the blends of P-120 with 50 wt% of EVA-15, EVA-20 and EVA-28.

Correspondingly, as shown in Fig. 7, the storage modulus of the blends varied drastically between 0°C and 25°C, and the loss modulus of the blends had peaks at 19°C, 27°C and at 24°C for EVA-15, EVA-20 and EVA-28, respectively. At higher temperatures, the modulus was found to increase upon increasing vinyl acetate content in the EVA. This proves the fact that crystallites that behave as rigid fillers in an amorphous matrix have moduli, compared with the rubbery amorphous. Also, we could not decide of miscibility for all blends from Figs. 5–7.

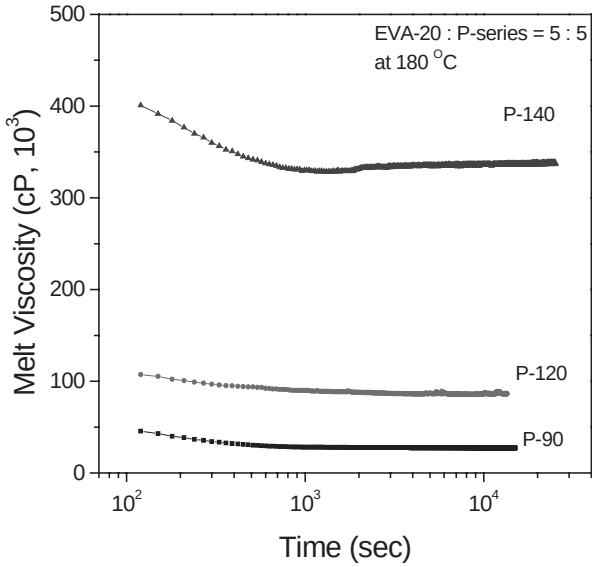

Fig. 8. Melt viscosity of EVA-20 blends with 50 wt% of P-90, P-120 and P-140 at 180°C as a function of time.

3.3. Melt viscosity

For the manufacture of hot-melt adhesives, the materials used need to be sufficiently stable both during storage and processing as well as during their application. In particular, the thermal stability of hot-melt adhesives is of major importance. Fig. 8 shows the melt viscosity of EVA-20 with P-90, P-120 and P-140 at 180°C as a function of time. Decrease of melt viscosity means thermal degradation of the adhesive. The increase of viscosity at the application temperature develop problems for the end user of the adhesive, resulting in unscheduled interruptions in production, because of plugged transfer lines and applicators [12]. At the beginning of the measurements, the melt viscosity was observed to slightly decrease, however subsequently the melt viscosities of the blend became stabilized. In this study, the melt viscosities were compared at 900 s. The viscosity was affected by molecular weight, annealing temperature, vinyl acetate content and concentration [13,14]. Fig. 9 shows the melt viscosity as a function of the softening point of the aromatic hydrocarbon resin at 160°C, 180°C and 200°C, respectively. The melt viscosity decreased with increasing temperature and decreasing softening point of the aromatic hydrocarbon resin. The blend of EVA-20 with P-140 shows a relatively high melt viscosity. Its melt viscosity is about 10 times that of the blend of EVA-20 with P-90, because P-140 has a higher molecular weight than the other aromatic hydrocarbon resins in Table 2. This proved that molecular weight, softening point and viscosity has an effect on the alkyl groups of aromatic hydrocarbon resin. Fig. 10 shows the melt viscosity of EVA-20 for different blend ratios. A rubbery polymer provides the

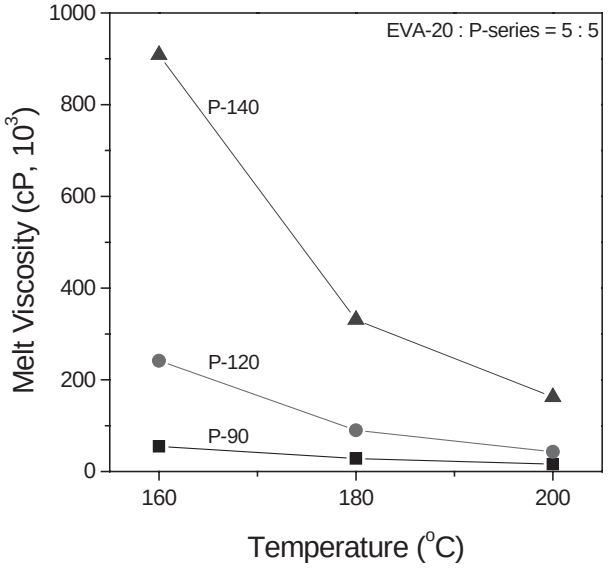

Fig. 9. Melt viscosity of EVA-20 blends with P-90, P-120 and P-140 at 160°C, 180°C and 200°C.

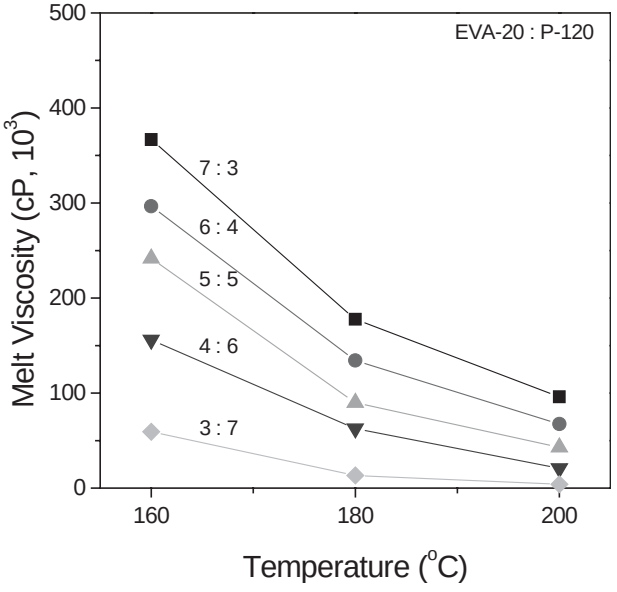

Fig. 10. Melt viscosity of EVA-20 blends with P-120 as a function of the blend ratio at 160°C, 180°C and 200°C.

elastic component, while a low molecular weight tackifying resin constitutes the viscous component [9]. Thus, the melt viscosity decreased as the content of the aromatic hydrocarbon resin increased, since the content of the low molecular weight aromatic hydrocarbon resins increase. Chung et al. [15] have reported similar behavior in the case of polyamide/terpene resin blends. Fig. 11 shows the melt viscosity of P-120 with EVAs which have different vinyl acetate contents at 160°C, 180°C and 200°C, respectively. The melt viscosity decreased with increasing temperature and VAc content.

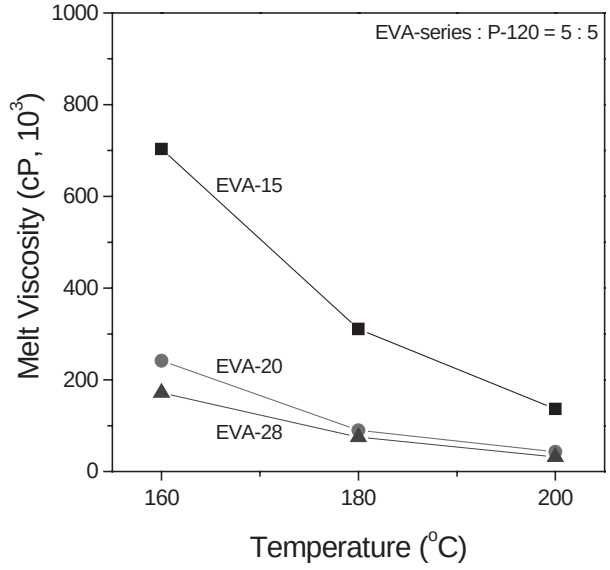

Fig. 11. Melt viscosity of P-120 blends with 50wt% of EVA-15, EVA-20 and EVA-28 at 160°C, 180°C and 200°C.

The results for these P-120 blends are similar to the results shown in Figs. 9 and 10. The EVA-15 blend shows a very high melt viscosity compare with the other blends because EVA-15 has a relatively high molecular weight or melt index compared to the other EVAs. Increasing the softening point of the aromatic hydrocarbon resin and its molecular weight increase the melt viscosity of the resultant blend. However, increasing the VAc content of the EVA caused the melt viscosity to decrease, in cases where the melt indices were the same or similar. Suitable melt viscosity depends on application, but low melt viscosity can lower the application temperature. Generally, improving the wetting of an adhesive requires that its melt viscosity be decreased, while its mechanical properties are decreased. Nevertheless, if its mechanical properties can be increased simultaneously with an improvement in its wetting properties, then this is even better.

3.4. Wide angle X-ray scattering

Wide angle X-ray scattering (WAXS) is used to provide information such as whether the polymer is crystalline or amorphous, whether it is oriented or unoriented, and the size of any repeat distance. In addition, structural information such as the unit cell, space group and full structure of a crystalline or semicrystalline polymer can be determined. However, for non-crystalline polymers the information that can be obtained is limited [16].

The X-ray diffraction patterns of the EVA/aromatic hydrocarbon resin blends as a function of the blend ratio are shown in Fig. 12. It is evident from the figure that there is one intense broad reflection at 21.1° (2θ),

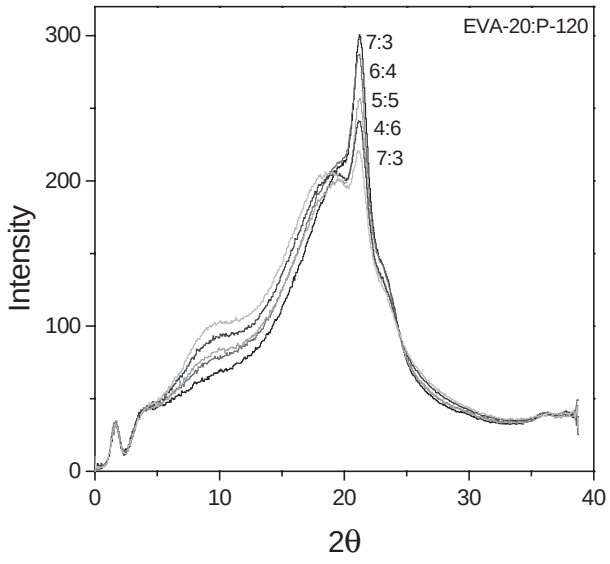

Fig. 12. X-ray diffraction patterns of EVA/aromatic hydrocarbon resin blends as a function of the blend ratio.

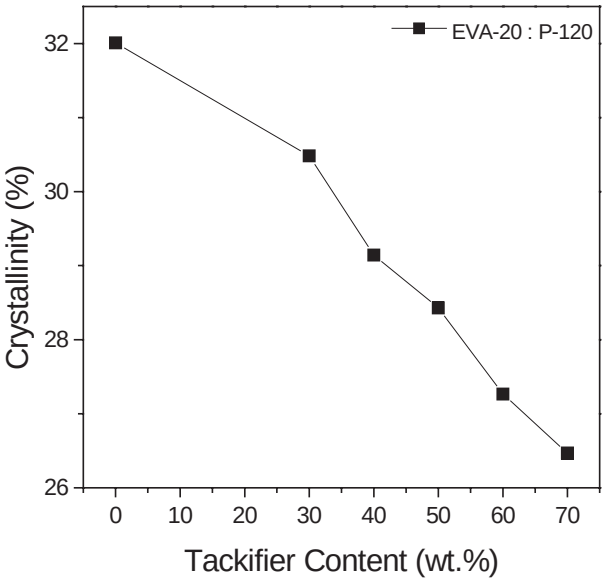

Fig. 13. Crystallinity of EVA-20 blends with P-120 as a function of the blend ratio.

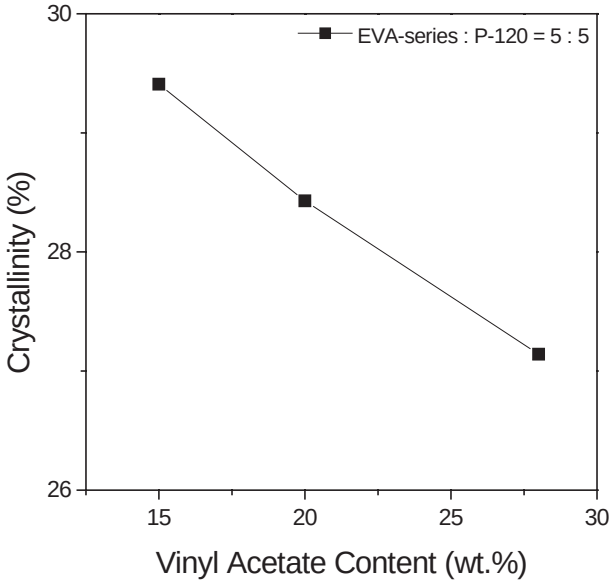

Fig. 14. Crystallinity of P-120 blends with 50 wt% of EVA-15, EVA-20 and EVA-28.

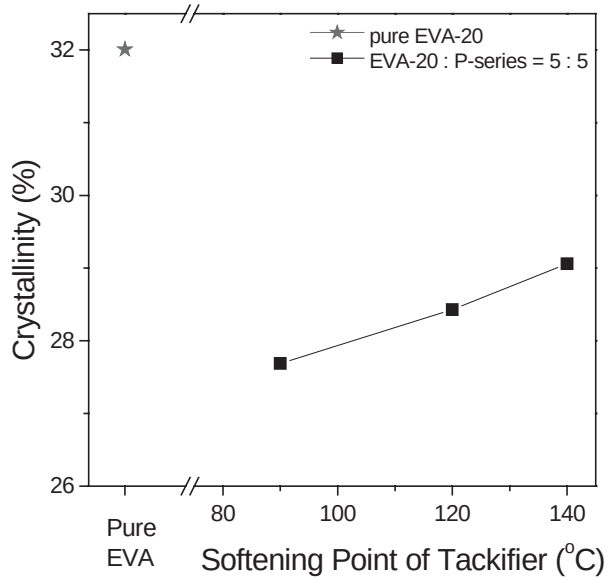

Fig. 15. Crystallinity of EVA-20 blends with 50 wt% of P-90, P-120 and P-140.

which suggests that the diffraction could be attributed to the presence of an amorphous region. Fig. 13 shows the crystallinity of the blend of EVA-20 with P-120 as a function of the blend ratio. The addition of aromatic hydrocarbon resin decreases the crystallinity because portion of EVA decreased. The crystallinity of the blend of P-120 with 50 wt% of EVA-15, EVA-20 and EVA-28 is given in Fig. 14. This result is similar to that of DSC in Figs. 1 and 4. Increasing the VAc content decreases the crystallinity of the blend. This is due to the effect of the increasing VAc content, which causes the crystalline region of ethylene to decrease. Fig. 15 shows the crystallinity of the blend of EVA-20 with 50 wt% of aromatic hydrocarbon resin with different softening points. In cases where the blend ratio is the same, increasing the softening point of the aromatic hydrocarbon resin increases the crystallinity.

3.5. Single lap-shear strength

Fig. 16 shows the single lap-shear strength of the blend of EVA-20 with 50 wt% of P-90, P-120 and P-140 at a crosshead speed of 300 mm/min and at a

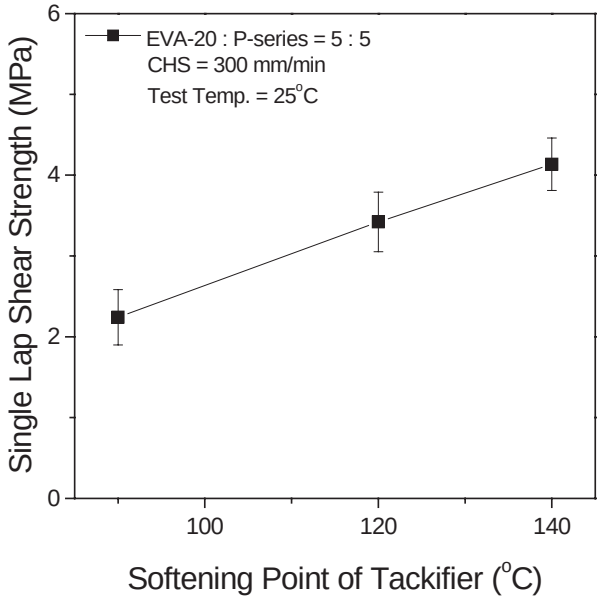

Fig. 16. Single lap-shear strength of the blend of EVA-20 with 50 wt% of P-90, P-120 and P-140.

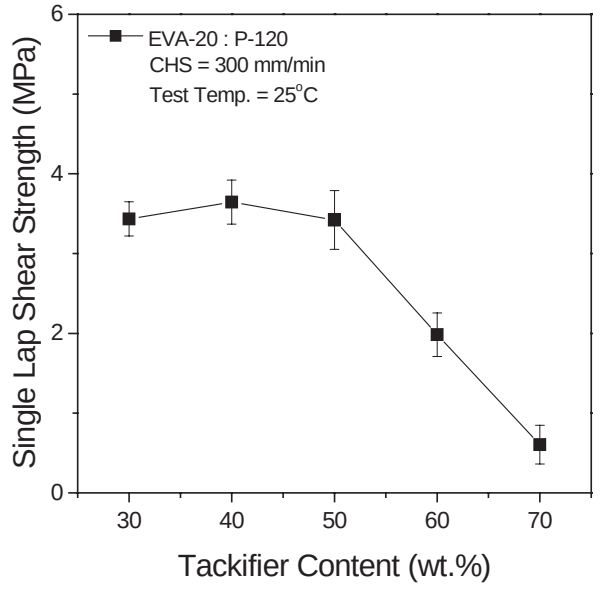

Fig. 17. Single lap-shear strength of the blend of EVA-20 with P-120 as a function of blend ratio.

temperature of 25°C. Single lap-shear strength increased with increasing the softening point of the aromatic hydrocarbon resin. Fig. 17 shows the single lap-shear strength of the blend EVA-20 with P-120 as a function of blend ratio. The single lap-shear strength increased up to 40 wt% of aromatic hydrocarbon resin, then, decreased, because the blend becomes more brittle as the concentration of aromatic hydrocarbon resin is increased. Fig. 18 shows the single lap-shear strength of the blend of P-120 with 50 wt% of EVA-15, EVA-20 and

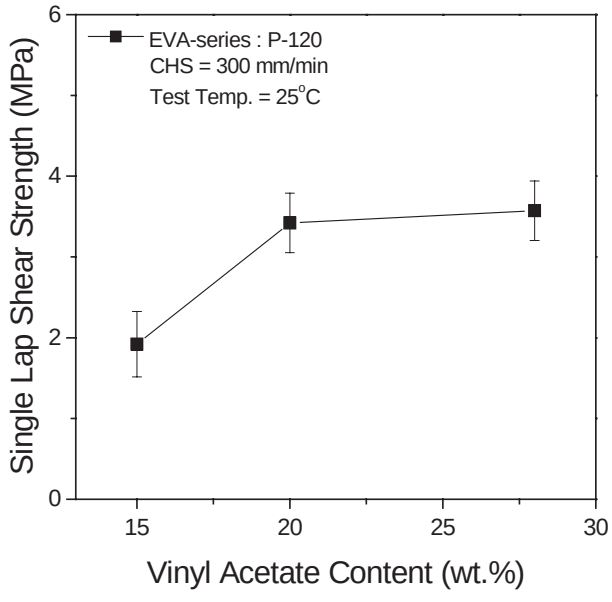

Fig. 18. Single lap-shear strength of the blend of P-120 with 50 wt% of EVA-15, EVA-20 and EVA-28.

EVA-28. The single lap-shear strength increased up to 20 wt% of VAc content, then, it very slightly increased.

3.6. Failure mode

Failure modes following the single lap-shear test were divided into interfacial, interfacial–cohesive and cohesive failure. Interfacial failure signifies failure at the adherend/blend interface. Interfacial–cohesive failure (or mixed failure) has interfacial failure and cohesive failure. Cohesive failure occurs when the adhesive remains on both adherends [17,18].

Fig. 19 shows pictures of the failure surface of the blend of EVA-20 with P-90, P-120 and P-140. There was an increasing tendency for cohesive failure to occur with increasing softening point of the aromatic hydrocarbon resin. Also, Fig. 20 shows pictures of the failure surface of the blend of EVA-20 with P-120 as a function of blend ratio. The tendency for interfacial failure mode to occur decreased with increasing aromatic hydrocarbon resin content. The failure mode as a function of the vinyl acetate content is given in Fig. 21, and these results are similar to those of Figs. 19 and 20. There was an increasing tendency for cohesive failure to occur with increasing vinyl acetate content.

4. Conclusion

Measurements of the glass transition temperatures of the blends were conducted using DSC. Pure components, EVAs and aromatic hydrocarbon resins, show clear glass transition temperatures and melting peaks.

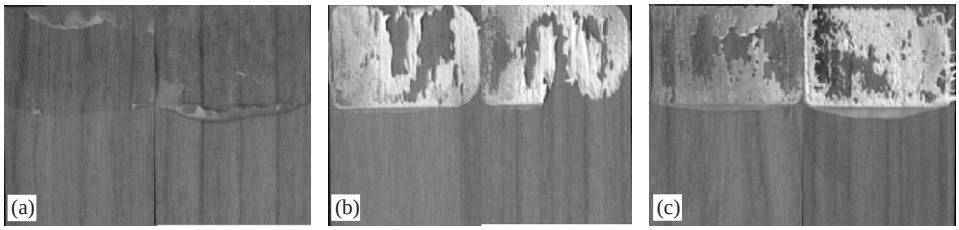

Fig. 19. Optical pictures of the failure surface of EVA-20 blends with 50 wt% of P-90, P-120 and P-140.

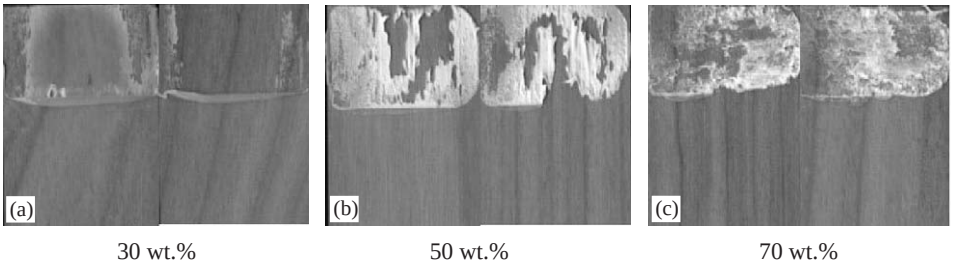

Fig. 20. Optical pictures of the failure surface of EVA-20 blends with P-120 as a function of the blend ratio.

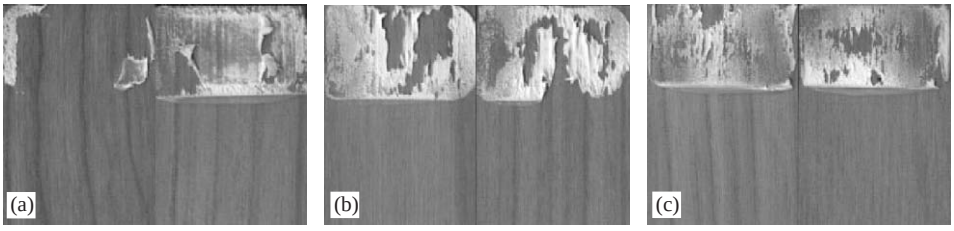

Fig. 21. Optical pictures of the failure surface of the blends of P-120 with 50 wt% of EVA-15, EVA-20 and EVA-28.

For the blends, the glass transitions are observed in the range of $-30^{\circ}C$ to $-20^{\circ}C$. However, it is difficult to identify the glass transition temperatures in the high temperature region, because of the melting peaks of the EVAs.

The storage modulus of the blends varied drastically between $0^{\circ}C$ and $25^{\circ}C$ in all blends. Also, the peaks of loss modulus increased with increasing softening point of the aromatic hydrocarbon resin.

The melt viscosity of all of the blends decreased with increasing temperature. It increased with increasing softening point of the aromatic hydrocarbon resin, but decreased with increasing aromatic hydrocarbon resin and vinyl acetate content.

The addition of aromatic hydrocarbon resin decreased the crystallinity. However, in cases of the same blend ratio, crystallinity increased with increasing the softening point of the aromatic hydrocarbon resin. Also, increasing the vinyl acetate content decreased the crystallinity of the blend, due to the effect of the increasing vinyl acetate content, which caused the crystalline region of ethylene to decrease.

Single lap-shear strength of the hot-melt adhesives increased with increasing softening point of the aromatic hydrocarbon resin and vinyl acetate content. Also, the single lap-shear strength increased up to 40 wt% of aromatic hydrocarbon resin, and then decreased. The tendency for cohesive failure occurred with increasing softening point of the aromatic hydrocarbon resin, concentration of the aromatic hydrocarbon resin and vinyl acetate content.

Acknowledgement

This work was supported in part by the Brain Korea 21 Projects in 2003.

References

[1] Hu AT, Tsai RS, Lee YD. J Appl Polym Sci 1989;37:1863.
[2] Jarvis NR. Adhesives Age 1995;38:26.

[3] Turreda LD, Sekiguchi Y, Takemoto M, Kajiyama M, Hatano Y, Mizumachi H. J Appl Polym Sci 1998;70:409.
[4] Shin HH, Hamed GR. J Appl Polym Sci 1997;63:323.
[5] Shin HH, Hamed GR. J Appl Polym Sci 1997;63:333.
[6] Chen X, Zhong H, Jia L, Tang R, Qiao J, Zhang Z. Int J Adhes Adhes 2001;21:221.
[7] Sunwoo KI, Hong YH. Polym Sci Technol Korea 1995;6:577.
[8] Schlademan JA. In: Satas D, editor. Handbook of pressure sensitive adhesive technology. Rhode Island: Warwick; 1989.
[9] Gierenz G, Karmann W. Adhesives and adhesive tapes. Weinheim: Wiley-VCH; 2001.
[10] Chen X, Zhong H, Jia L, Tang R, Qiao J, Zhang Z. J Appl Polym Sci 2001;81:2696.
[11] Rasmussen JK, Smith II HK. J Appl Polym Sci 1983;28:2473.
[12] Colegrove LF, Clay W, Genova RD. 1998 Hot melt symposium, Tappi. 1998. p. 1.
[13] Qian JW, Qi GR, Cheng RS. Eur Polym J 1997;33:1263.
[14] Qian JW, Qi GR, Cheng RS. Eur Polym J 1997;34:445.
[15] Chung KH, Hong YK, Chun YS. J Korean Ind Eng Chem 1998;9:226.
[16] Vickers ME. In: Richards RW, editors. Scattering methods in polymer science. New York: Ellis Horwood; 1995.
[17] Campbell D, White JR. Polymer characterization. New York: Chapman & Hall; 1989.
[18] Pocius AV. Adhesion and adhesives technology, 2nd ed. Cincinnati: Hanser; 2002.